Characterisation of a Monolithic 3D-printed Tactile Sensor Using an SSIM-based Analysis

Xiaoqing Guo, Nathan F. Lepora*, Efi Psomopoulou*

I. INTRODUCTION

Vision-based tactile sensors capture deformation through optical imaging, enabling high spatial resolution beyond conventional electronic tactile sensing[1]. The TacTip family provides a biomimetic design based on a soft skin, internal pins, and marker tracking [2], and has already been applied in tactile servoing, object manipulation, and related dexterous interaction tasks[3]–[6]. However, conventional TacTip sensors require multi-step fabrication, including gel injection, which introduces variability and increases complexity.

In this work, we present a monolithic 3D-printed TacTip-like tactile sensor in which the compliant gel is replaced by a directly printed soft transparent solid, enabling single-cycle fabrication. To characterize its behavior, indentation experiments are performed and deformation is quantified using the structural similarity index (SSIM), a structure-preserving image similarity metric that is well suited to vision-based tactile sensing and has been adopted in prior tactile perception studies [3], [7]–[10]. Results show that pin length and gel thickness strongly influence the response, corresponding to mechanical deformation transmission and optical amplification through refraction.

The main contributions are:

- A monolithic 3D-printed tactile sensor eliminating gel injection via a soft transparent solid.
- An SSIM-based framework for quantifying deformation from image similarity.
- Experimental identification of two governing mechanisms: pin length controls mechanical transmission, while effective gel thickness governs optical amplification through refraction.

II. METHODOLOGY

A. Sensor Design and Fabrication

Fig. 1 shows the structure of the proposed tactile skin. The sensor inherits the basic TacTip architecture, including a skin, pins, marker layer, gel region, window, and cradle. Unlike the conventional TacTip, however, the compliant internal region is fabricated directly in a monolithic 3D-printing process, eliminating the gel-injection step.

Flexible Agilus material is used for the skin and pins, while rigid Vero materials are used for the marker layer and window. To improve optical clarity, a thin transparent UV resin coating is applied to the printed window after fabrication. Several sensor configurations were fabricated by varying gel thickness and pin length. Thicker gel and shorter pins generally improved compliance, whereas excessive gel thickness reduced marker visibility because of accumulated 3D-printing textures inside the soft material. In our experiments, the markers remained clearly visible when the distance t between the marker plane and the gel surface was no greater than $4\,\mathrm{mm}$. Therefore, ten skin configurations were designed to balance compliance and marker visibility. The first group ($t = 2\,\mathrm{mm}$) includes gel4–pin2, gel5–pin3, and gel6–pin4; the second group ($t = 3\,\mathrm{mm}$) consists of gel5–pin2, gel6–pin3, and gel7–pin4; and the third group ($t = 4\,\mathrm{mm}$) covers gel5–pin1, gel6–pin2, gel7–pin3, and gel8–pin4.

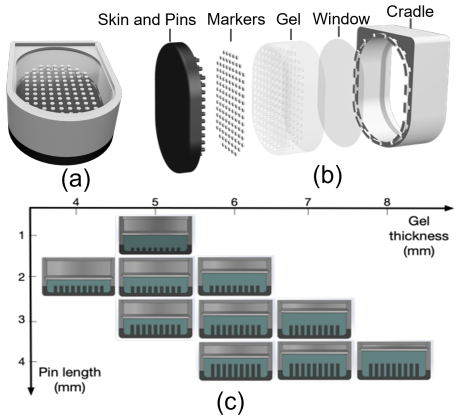

Fig. 1. Structure of the proposed tactile skin

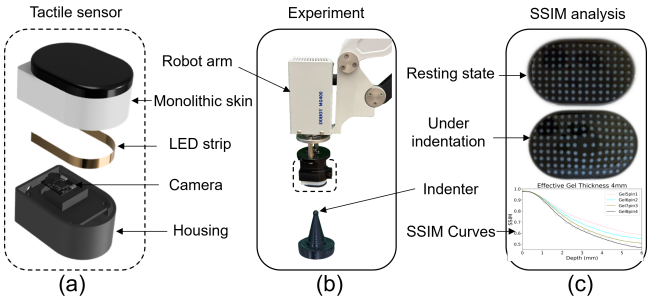

Fig. 2. Overview of the sensor design, experimental setup, and SSIM-based analysis.

B. Experimental Design

Fig. 2 summarises the proposed sensor, the indentation experiment, and the SSIM-based analysis pipeline.Indentation

Authors are with the School of Engineering Mathematics and Technology, and Bristol Robotics Laboratory, University of Bristol, U.K. (emails: xq.guo@bristol.ac.uk, n.lepora@bristol.ac.uk, efi.psomopoulou@bristol.ac.uk, *co-supervisors).

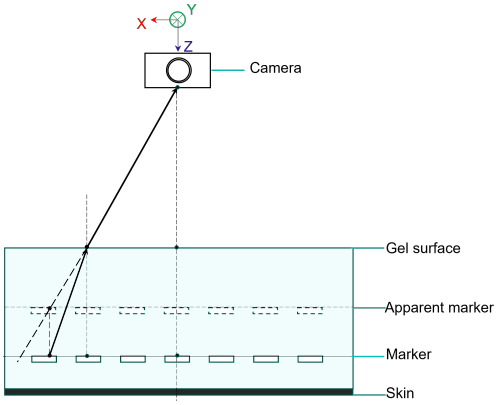

Fig. 3. Refraction modifies effective imaging geometry.

experiments were performed to study normal deformation of the Mono3D-TacTip. A sphere-tipped indenter was driven vertically into the center of the tactile surface in increments of 0.1 mm. At each depth, tactile images were acquired five times under controlled lighting conditions, and the repeated measurements were averaged to reduce noise.

Ten sensor configurations were tested, combining different gel thicknesses and pin lengths. Since these parameters also affect optical imaging through refraction, the sensors were grouped using the effective gel thickness t:

$$t = D_{\text{gel}} - L_{\text{pin}}, \tag{1}$$

where D_{gel} is the gel thickness and L_{pin} is the pin length. Fig. 3 illustrates that refraction inside the gel modifies the effective imaging geometry. Under a paraxial approximation, the pinhole imaging relationship remains linear and can be written as

$$x_{\text{true}} = (1-k)x_{\text{app}}, \tag{2}$$

where

$$k = \frac{D_{\text{gel}} - L_{\text{pin}}}{D - L_{\text{pin}}}\left(1 - \frac{1}{n}\right), \tag{3}$$

where x_{true} is the true lateral position, x_{app} is the apparent lateral position obtained when refraction is ignored, D is the axial distance between the camera pinhole and the skin plane, n is the refractive index of the gel, and k is the refraction influence factor.

C. SSIM-Based Deformation Quantification

To quantify tactile deformation, each image acquired during indentation was compared with a no-contact reference image using the structural similarity index (SSIM) [11]. For each depth, five SSIM values were obtained and averaged to construct an SSIM–depth response curve.

The measured curves were fitted using a double-Gaussian model to capture the asymmetric decay of SSIM with indentation depth.

$$\text{SSIM}(d) = A_1 \exp\left(-\frac{d^2}{2\sigma_1^2}\right) + A_2 \exp\left(-\frac{(d-\mu_2)^2}{2\sigma_2^2}\right) + C. \tag{4}$$

where $\text{SSIM}(d)$ denotes the structural similarity index at indentation depth d, A_1 and A_2 denote the amplitudes of the two Gaussian components, μ_2 is their characteristic depth,

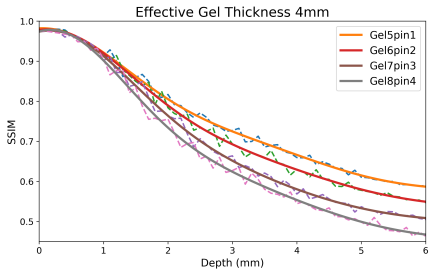

Fig. 4. Representative SSIM–depth curves and double-Gaussian fitting results for proposed sensors with different pin lengths.

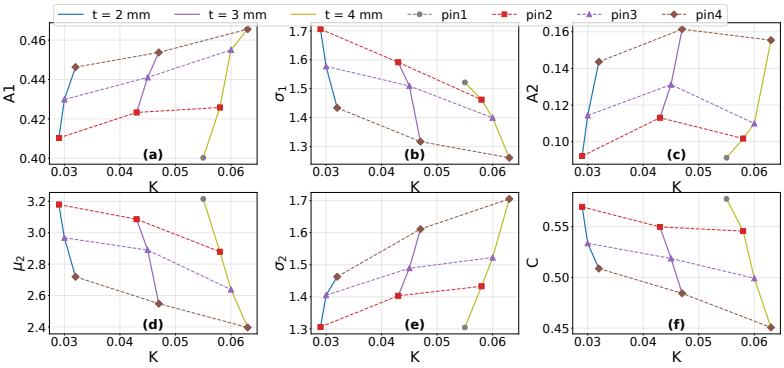

Fig. 5. Variation of the fitted parameters with respect to the refraction influence factor K.

σ_1 and σ_2 control the spatial extents (spreads) of the two components, and C represents a baseline SSIM offset.

III. RESULTS

Fig. 4 shows that SSIM decreases monotonically with indentation depth, while the decay profile depends strongly on structural design. Fig. 5 further summarizes the variation of fitted parameters with respect to the refraction influence factor.

For fixed effective gel thickness, increasing pin length leads to systematic parameter changes. The near-surface amplitude A_1 increases monotonically, indicating stronger deformation transmission and a steeper initial SSIM drop. Meanwhile, σ_1 decreases, suggesting a more localized near-surface response. The parameter A_2 also increases but remains significantly smaller than A_1, indicating that deep deformation contributes as a secondary effect. In addition, μ_2 decreases and σ_2 increases, showing that the dominant deformation response occurs earlier and becomes more spatially distributed.

For fixed pin length, increasing effective gel thickness primarily affects the optical response. The amplitude A_1 increases due to stronger refractive amplification, while μ_2 decreases and σ_1 becomes smaller, indicating earlier and sharper SSIM degradation. In contrast, σ_2 increases, suggesting a more gradual decay at larger depths.

These results indicate that pin length governs mechanical deformation transmission, whereas effective gel thickness controls optical amplification through refraction.

REFERENCES

[1] H. Li, Y. Lin, C. Lu, M. Yang, E. Psomopoulou, and N. F. Lepora, "Classification of vision-based tactile sensors: A review," *IEEE Sensors Journal*, vol. 25, no. 19, pp. 35 672–35 686, 2025.

[2] B. Ward-Cherrier, N. Pestell, L. Cramphorn, B. Winstone, M. E. Giannaccini, J. Rossiter, and N. F. Lepora, "The TacTip family: Soft optical tactile sensors with 3d-printed biomimetic morphologies," *Soft robotics*, vol. 5, no. 2, pp. 216–227, 2018.

[3] C. J. Ford, H. Li, J. Lloyd, M. G. Catalano, M. Bianchi, E. Psomopoulou, and N. F. Lepora, "Tactile-driven gentle grasping for human-robot collaborative tasks," *arXiv preprint arXiv:2303.09346*, 2023.

[4] Y. Lin, A. Church, M. Yang, H. Li, J. Lloyd, D. Zhang, and N. F. Lepora, "Bi-touch: Bimanual tactile manipulation with sim-to-real deep reinforcement learning," *IEEE Robotics and Automation Letters*, vol. 8, no. 9, pp. 5472–5479, 2023.

[5] M. Yang, Y. Lin, A. Church, J. Lloyd, D. Zhang, D. A. Barton, and N. F. Lepora, "Sim-to-real model-based and model-free deep reinforcement learning for tactile pushing," *IEEE Robotics and Automation Letters*, vol. 8, no. 9, pp. 5480–5487, 2023.

[6] Y. Lin, B. Deng, K. Pu, C. Lu, M. Yang, E. Psomopoulou, and N. F. Lepora, "Neuraltouch: Neural descriptors for precise sim-to-real tactile robot control," *IEEE/ASME Transactions on Mechatronics*, 2026.

[7] J. W. James, A. Church, L. Cramphorn, and N. F. Lepora, "Tactile model o: Fabrication and testing of a 3d-printed, three-fingered tactile robot hand," *Soft Robotics*, vol. 8, no. 5, pp. 594–610, 2021.

[8] N. F. Lepora, C. Ford, A. Stinchcombe, A. Brown, J. Lloyd, M. G. Catalano, M. Bianchi, and B. Ward-Cherrier, "Towards integrated tactile sensorimotor control in anthropomorphic soft robotic hands," in *2021 IEEE international conference on robotics and automation (ICRA)*. IEEE, 2021, pp. 1622–1628.

[9] E. Psomopoulou, N. Pestell, F. Papadopoulos, J. Lloyd, Z. Doulgeri, and N. F. Lepora, "A robust controller for stable 3d pinching using tactile sensing," *IEEE Robotics and Automation Letters*, vol. 6, no. 4, pp. 8150–8157, 2021.

[10] J.-T. Lee, D. Bollegala, and S. Luo, ""touching to see" and "seeing to feel": Robotic cross-modal sensory data generation for visual-tactile perception," in *2019 International conference on robotics and automation (ICRA)*. IEEE, 2019, pp. 4276–4282.

[11] Z. Wang, A. C. Bovik, H. R. Sheikh, and E. P. Simoncelli, "Image quality assessment: from error visibility to structural similarity," *IEEE transactions on image processing*, vol. 13, no. 4, pp. 600–612, 2004.